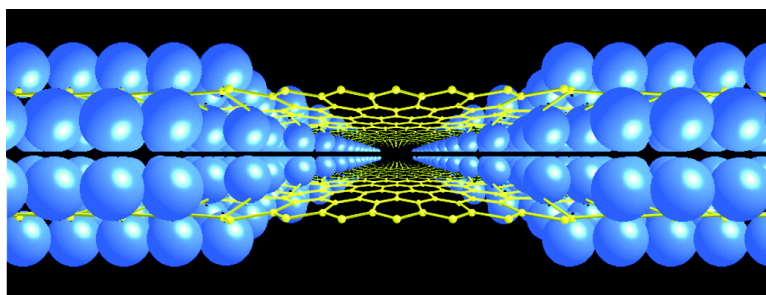


Electronics and Magnetism of Patterned Graphene Nanoroads

Abhishek K. Singh, and Boris I. Yakobson

Nano Lett., **2009**, 9 (4), 1540-1543 • DOI: 10.1021/nl803622c • Publication Date (Web): 18 March 2009

Downloaded from <http://pubs.acs.org> on April 14, 2009



More About This Article

Additional resources and features associated with this article are available within the HTML version:

- Supporting Information
- Access to high resolution figures
- Links to articles and content related to this article
- Copyright permission to reproduce figures and/or text from this article

[View the Full Text HTML](#)

Electronics and Magnetism of Patterned Graphene Nanoroads

Abhishek K. Singh and Boris I. Yakobson*

Department of Mechanical Engineering and Materials Science, and Department of Chemistry, Rice University, Houston Texas 77005

Received November 29, 2008; Revised Manuscript Received February 11, 2009

ABSTRACT

Individual ribbons of graphene show orientation-dependent electronic properties of great interest, yet to ensure their perfect geometry and integrity or to assemble free ribbons into a device remains a daunting task. Here we explore, using density functional theory, an alternative possibility of “nanoroads” of pristine graphene being carved in the electrically insulating matrix of fully hydrogenated carbon sheet (graphane). Such one-dimensional entities show individual characteristics and, depending upon zigzag (and their magnetic state) or armchair orientation, can be metallic or semiconducting. Furthermore, the wide enough zigzag roads become magnetic with energetically similar ferro- and antiferromagnetic states. Designing magnetic, metallic, and semiconducting elements within the same mechanically intact sheet of graphene presents a new opportunity for applications.

Graphene, a single layer of carbon atoms arranged in a honeycomb lattice, has been the focus of recent research, due to its unique zero-gap electronic structure, which leads to massless charge carriers. As a consequence of this, graphene exhibits a variety of exciting phenomena¹ such as anomalous quantum Hall effect, ballistic transport, and large coherence length. Rapid progress has been made recently in producing and separating individual graphene sheets.^{2–5} These developments have paved the way for a range of nanodevices that conceptually can be fabricated by altering the electronic properties of graphene.

Notably, graphene nanoribbons (GNR)^{6–9} offer a possibility of achieving tunable electronic properties. GNRs are synthesized by cutting the graphene sheets and passivating the edge carbon atoms (e.g., by hydrogen). Depending upon the width and orientation of the edges, the GNRs can be semiconducting or metallic.^{10–14} The zigzag GNRs are shown to be magnetic^{15–20} and an application of electric field renders them half-metallic,^{18,20,21} where only one of the spin channels conducts, while the other remains insulating. Half-metallicity in zigzag GNRs is promising for spintronic devices. There remain several major obstacles to overcome before GNRs can be utilized as promised. Producing graphene ribbons with zigzag or armchair edges in a controlled fashion is still a challenge. Furthermore, integrating the semiconducting and metallic ribbons to form devices is hard as well, and even manipulation of very flexible ribbons must require extreme dexterity. Some of these difficulties can possibly be circumvented by another approach, which does not require cutting mechanically free and therefore easily deformable, “flimsy”

nanoribbons.²² Recent studies^{23,24} on hydrogenation of graphene show two important aspects: (i) a fully hydrogenated graphene is a wide gap semiconductor, and (ii) it should form very sharp interfaces²⁴ with the pristine graphene in the same plane. Can hydrogenation be utilized to form the geometrical areas, especially “roads”, of pristine graphene with the desired electronic properties embedded in fully hydrogenated phase without the need for cutting?^{8,25} We explore these using ab initio calculations to support the proposal to pattern the pristine graphene nanoroads (GNR', henceforth marked with a “prime” to distinguish from similar acronym for the nanoribbons) via selective hydrogenation of the graphene sheets. We show that the electronic properties of the GNR's depend sensitively upon their orientations, widths, and magnetic states, essentially providing the tunability that can be utilized in several devices with varying application. Most importantly, the semiconducting as well as metallic GNR's can be patterned on the same graphene sheet thereby taking care of integration automatically.

The nanoroads can be formed via partial hydrogenation of graphene sheet as shown in Figure 1. Following ref 21, the armchair and zigzag nanoroads (AGNR' and ZGNR') are classified by number of pristine (in sp^2 state) dimer lines and zigzag chains N_a and N_z , respectively, Figure 1. The lowest energy structure of hydrogenated graphene is achieved when H-atoms are attached from both sides, due to the following reasons. After the adsorption of the first hydrogen, which breaks the pairing of π -electrons between two subgroups of starred and unstarred carbon atoms, the system is left with an unpaired π -electron.²⁶ We have seen²⁴ that adding another hydrogen to the carbon atom from the other

* To whom correspondence should be addressed. E-mail: biy@rice.edu.

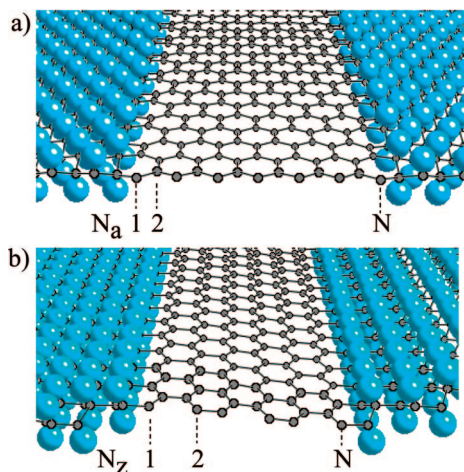


Figure 1. Relaxed structure of (a) armchair and (b) zigzag nanoroads. The width is measured by the number of pristine sp^2 -carbon dimer-lines (N_a) or zigzag chains (N_z), respectively.

subgroup removes the radical thereby lowering the energy. Additionally, adsorption of H changes of course the hybridization of carbon from sp^2 to sp^3 that leads to buckling of hydrogenated carbon. When the two adjacent carbon atoms are hydrogenated from the opposite sides, the induced strains compensate each other, which further reduces the energy. Driven by these two effects, the hydrogenation of graphene from both sides is preferred, which eventually leads to formation of hydrogenated phase²⁴ of stoichiometry CH, with the distinct boundary-interface separating it from the pristine graphene area. Similar tendency has been observed in the case of binding of graphene on metal surfaces;²⁷ it has been shown that graphene does not bind to metal surfaces, unless metal is deposited on the other side of the graphene, thus facilitating the sp^3 transformation of graphene, which effectively becomes a monolayer slab of diamond.

The electronic structure calculations are performed using density functional theory based pseudopotential plane-wave method as implemented in VASP.^{28,29} The ion-electron interactions are treated with the projected augmented wave (PAW) pseudopotentials^{30,31} using the Perdew-Burke-Ernzerhof exchange-correlation functional³² for the spin-polarized generalized gradient correction. Reciprocal space integrations are carried out at $1 \times 1 \times 10$ Monchorst-Pack k-grids. Symmetry unrestricted optimizations of both geometry and spin are performed using the conjugate gradient scheme until the force components on every atom are less than 0.005 eV/Å. Standard tests with respect to k-points sampling and plane-wave energy cut-offs are carried out to ensure the reliability of the method. Periodic boundary condition (PBC) is employed and unitcell lengths along the roads are optimized. The in-plane unitcell lengths across the road are taken large enough to avoid the spurious interactions with the images. Likewise, 15 Å of vacuum is added in the direction normal to the plane.

The overall effect of relaxation on the geometry of the two types of GNR's differs. The relaxed AGNR's are completely flat; see Figure 1a. The alternate C atoms bonded to hydrogen move out of the plane in opposite directions

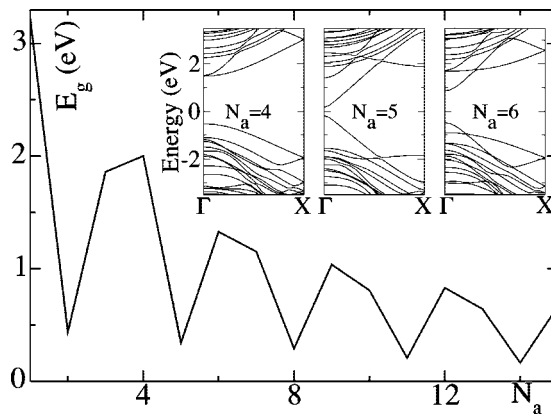


Figure 2. The band gap variation for AGNR's as a function of the width N_a . Inset: band structures of 4-, 5-, and 6-AGNR'.

along the orientation of AGNR's, keeping the roads flat; see Figure 1. In the case of ZGNR's due to geometry, the alternating halves of the hydrogenated zigzag rings move in and out of the plane. As a result of that, the zigzag rings at the two interfaces relax in opposite directions, respectively, introducing an overall tilt, as shown in Figure 1b. With the increasing width of the ZGNR's, the tilt becomes more localized at the interface and part of the road away from the interface remains flat. In order to make sure that these tilts are not artifact of the relatively smaller width of the roads, we carry out calculation with very large unit cell including 18 pristine and hydrogenated zigzag chains (18-ZGNR'). This road also tilts, accompanied by an increase in the width of the flat part. In order to ensure that the tilt is not due to employing PBC in the perpendicular direction, a calculation on a road with the finite width of hydrogenated part has been performed. While the road tilts again at the interface, the overall system remains flat. Therefore the tilts in the ZGNR's are localized and originate from the geometry and are not caused by the PBC. Importantly though, the tilt has a very little effect on electronic and magnetic properties.

In order for the nanoroads to be well defined, the sharpness of the interfaces between hydrogenated and pristine graphene is important. Analysis shows that indeed the sharp interface has the lowest energy. We tested the robustness of these interfaces by calculating the energy cost of removing the hydrogen atom from the interface and placing them to the next C atom in adjacent zigzag chain (dimer line) in 18-ZGNR' (14-AGNR'). Upon relaxation in the 14-AGNR' the hydrogen moves back to the interface spontaneously, confirming the robustness of interface. In 18-ZGNR', although the H atom does not go back to the interface, the system becomes 2.32 eV higher in energy. Clearly, this energy cost to remove and displace the H is very large and cannot be overcome at the operational temperatures of the device.

We studied the electronic properties of the GNR's by calculating their band structure. The AGNR's are semiconductors with a band gap increasing for narrow AGNR's due to quantum confinement. Some of the semiconducting AGNR's have large band gaps, which can be tuned by controlling the width. Like in nanotubes and nanoribbons,

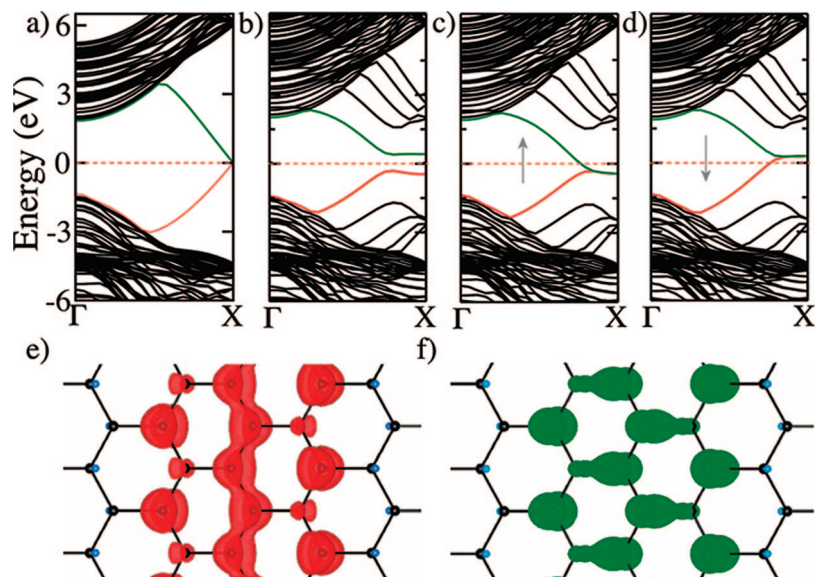


Figure 3. (a) The band structure of 1-ZGNR'. (b) The band structure of antiferromagnetic state of 5-ZGNR'. (c,d) The band structure of majority (c) and minority (d) spin channels of 5-ZGNR' in its ferromagnetic state. (e,f) The band-decomposed charge density corresponding to the lower (darker red) and upper (lighter green) bands in the vicinity of Fermi level of the 3-ZGNR'.

the gap here becomes very small for $N_a = 3p + 2$. The variation in band gap is not monotonous and can be subdivided into three families as shown in Figure 2. The band gaps in the three families follow hierarchy $\Delta_{3p+2} < \Delta_{3p+1} < \Delta_{3p}$ (except for the $N_a = 3$ and 4). This hierarchy is different from the one reported for the armchair nanoribbons.¹² The difference apparently comes from the nature of edges in the nanoribbons and interfaces in the GNR's: with a few exceptions,^{19,33,34} the edges of the nanoribbons are passivated by single H and retain the sp^2 hybridization of C-atoms, while for the roads the interfaces are formed between sp^2 and sp^3 C-atoms.

The electronic structures of ZGNR's are distinctly different from AGNR's and depend on magnetic state. Very narrow 1- and 2-ZGNR' are nonmagnetic; their two bands near Fermi level do not cross, leaving a very small gap, as shown in Figure 3a. In 1-ZGNR' there is only one sp^2 -zigzag chain surrounded by the sp^3 phase, while in the 2-ZGNR' there are two sp^2 - sp^3 interfaces next to each other. From the $N_z = 3$ onward, a more general behavior emerges. Wider antiferromagnetic ZGNR's are semiconducting, and the band structures for the spin-up and spin-down are degenerate and equally populated (Figure 3b). The band gap is 0.7 eV for $N = 3$ and decreases for the wider roads, following the trend $\sim 1/N$, similar to nanoribbons.^{12,19} However, very close in energy wider ferromagnetic ZGNR's are metallic; see Figure 3c,d. As an example, band structures are shown in Figure 3c,d for 5-ZGNR', which is metallic for both spin up and down channels, and the two bands near the Fermi level cross. Interestingly, the metastable ferromagnetic state in nanoribbons has similar band structure.³⁵ Furthermore, in all the N_z -ZGNR' exactly N_z bands move toward the Fermi level and out of these, only two of them cross. We analyze the nature of these two crossing bands of ZGNR's by plotting their corresponding band-decomposed charge densities, as shown for 3-ZGNR' in Figure 3e,f. These are π -bands formed

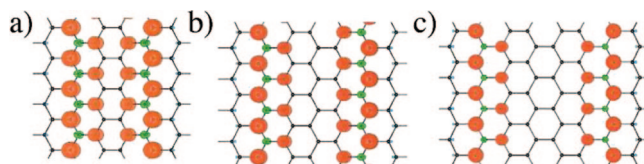


Figure 4. (a–c) The contour plots of the spin-density ($\rho_t - \rho_l$) of $N_z = 4$ -, 5-, and 6-ZGNR', respectively (red for positive and green for negative), in their ferromagnetic states. In the antiferromagnetic state, the colors at the two sp^2 - sp^3 interfaces must be inverted.

by the overlap of the p_z orbitals and mostly localized on the C atoms near the interfaces. Furthermore, these bands are very dispersive due to strong interactions among the p_z orbitals. This large dispersion also implies smaller effective masses for the charge carriers, which will lead to enhanced mobility and reduced resistivity.

Finally, we briefly discuss the magnetism in the nanoroads, as observed in spin-polarized calculations. All of the AGNR's and ZGNR's with $N_z < 3$ are nonmagnetic (bands corresponding to majority and minority spins are equally filled), while the rest of the ZGNR's are magnetic. According to our calculations, the ferro- and antiferromagnetic states are nearly degenerate (the differences are from 7 meV and less for wider GNR's, that is, within the error of computations). The total magnetic moment on all of the ferromagnetic ZGNR's is $0.80 \mu_B$ /unit cell and remains unchanged with the increasing width of the roads. As discussed above, the bands in the vicinity of the Fermi level are highly localized, which leads to the enhancement in exchange energy and helps to maintain the magnetism. We further analyzed the distribution pattern of the spin density. The isosurfaces of spin density of 4-, 5-, and 6-ZGNR's show their localized nature, as these are mostly concentrated on carbon atoms in the two adjacent zigzag chains at the interfaces; see Figure 4a–c. These features are invariant among all the magnetic ZGNR's including the widest road (18-ZGNR') considered

in this study. In the antiferromagnetic state, the spins are inverted on the one side relative to another across the road. The energy difference between the magnetic (either ferro- or antiferro-) and nonmagnetic states increases with the increasing width and saturates (~ 110 meV) at 6-ZGNR', similar to the trend reported for nanoribbons.^{19,35} Therefore, the magnetism in wider nanoroads should display better stability. Still, relatively smaller energy differences in the magnetic and nonmagnetic states of ZGNR's make their applications challenging.

In summary, we show that conducting and semiconducting nanoroads can in principle be patterned on a graphene by hydrogenation (or using other functional groups). One possibility is to achieve a rough pattern and directionality by the masked exposure to a reagent transforming sp^2 carbon into sp^3 , while further energy minimization of the interface (perhaps with some annealing stage) should ensure its atomic precision. The proposed AGNR's are semiconducting with the width-dependent band gaps (exhibiting smaller gaps at $N_a = 3p + 2$). The ZGNR's with $N_z > 2$ are magnetic with the ferro- and antiferromagnetic states of very similar energies. While antiferromagnetic state is semiconducting, the ferromagnetic state is metallic with a width-independent moment of $0.80 \mu_B$ /unit cell. The electronic properties of these roads show some analogy with that of carbon nanotubes and graphene nanoribbons; however, possibility of having metallic and semiconducting roads on the same planar geometry can be an advantage. Given the rapid progress made in the synthesis of isolated graphene sheets, the proposed patterning of the graphene has prospects to be achieved within the foreseeable time.

Acknowledgment. Authors are thankful to Arta Sadrzadeh and Enrique Muñoz for useful discussions. This work was supported by the Office of Naval Research (program managers Peter Schmidt and Kenny Lipkowitz) and partially by the AFRL Materials & Manufacturing Directorate. Computations were performed on the Rice Terascale Cluster and the Shared University Grid funded by NSF under Grant EIA-0216467.

Note Added in Proof: After the completion of this work, an experimental evidence of graphene hydrogenation was reported,^{36,37} further supporting the feasibility of the *nano-roads* approach described here.

References

- (1) Geim, A.; Novoselov, K. *Nat. Mater.* **2007**, *6*, 183.
- (2) Novoselov, K. S.; Geim, A. K.; Morozov, S. V.; Jiang, D.; Zhang, Y.; Dubonos, S. V.; Grigorieva, I. V.; Firsov, A. A. *Science* **2004**, *306*, 666.
- (3) Ohta, T.; Bostwick, A.; Seyller, T.; Horn, K.; Rotenberg, E. *Science* **2006**, *313*, 951.
- (4) Stankovich, S.; Dikin, D.; Dommett, G.; Kohlhaas, K.; Zimney, E.; Stach, E.; Piner, R.; Nguyen, S.; Ruoff, R. *Nature* **2006**, *442*, 282.
- (5) Zhang, Y.; Tan, Y.; Stormer, H.; Kim, P. *Nature* **2005**, *438*, 201.
- (6) Han, M. Y.; Ozyilmaz, B.; Zhang, Y.; Kim, P. *Phys. Rev. Lett.* **2007**, *98*, 206805.
- (7) Berger, C.; Song, Z.; Li, X.; Wu, X.; Brown, N.; Naud, C.; Mayou, D.; Li, T.; Hass, J.; Marchenkov, A. N.; Conrad, E. H.; First, P. N.; Heer, W. A. d. *Science* **2006**, *312*, 1191.
- (8) Ci, L.; Xu, Z.; Wang, L.; Gao, W.; Ding, F.; Kelly, K.; Yakobson, B. I.; Ajayan, P. *Nano Res.* **2008**, *1*, 116.
- (9) Chen, Z.; Lin, Y.; Rooks, M. J.; Avouris, P. *Physica E* **2007**, *40*, 228.
- (10) Cancado, L. G.; Pimenta, M. A.; Neves, B. R. A.; Medeiros-Ribeiro, G.; Enoki, T.; Kobayashi, Y.; Takai, K.; Fukui, K.; Dresselhaus, M. S.; Saito, R.; Jorio, A. *Phys. Rev. Lett.* **2004**, *93*, 047403.
- (11) Ezawa, M. *Phys. Rev. B* **2006**, *73*, 045432.
- (12) Son, Y.; Cohen, M.; Louie, S. *Phys. Rev. Lett.* **2006**, *97*, 216803.
- (13) Ezawa, M. *Physica E* **2008**, *40*, 1421.
- (14) Ezawa, M. *Phys. Rev. B* **2007**, *76*, 245415.
- (15) Fujita, M.; Wakabayashi, K.; Nakada, K.; Kusakabe, K. *J. Phys. Soc. Jpn.* **1996**, *65*, 1920.
- (16) Wakabayashi, K.; Fujita, M.; Ajiki, H.; Sigrist, M. *Phys. Rev. B* **1999**, *59*, 8271.
- (17) Barone, V.; Hod, O.; Scuseria, G. E. *Nano Lett.* **2006**, *6*, 2748.
- (18) Hod, O.; Barone, V.; Peralta, J. E.; Scuseria, G. E. *Nano Lett.* **2007**, *7*, 2295.
- (19) Kudin, K. N. *ACS Nano* **2008**, *2*, 516.
- (20) Hod, O.; Barone, V.; Scuseria, G. E. *Phys. Rev. B* **2008**, *77*, 035411.
- (21) Son, Y.; Cohen, M.; Louie, S. *Nature* **2006**, *444*, 347.
- (22) Bets, K.; Yakobson, B. *Nano Res.* **2009**, *2*, 161.
- (23) Sofo, J.; Chaudhari, A.; Barber, G. *Phys. Rev. B* **2007**, *75*, 153401.
- (24) Lin, Y.; Ding, F.; Yakobson, B. I. *Phys. Rev. B* **2008**, *78*, 041402.
- (25) Ajayan, P. M.; Yakobson, B. I. *Nature* **2006**, *441*, 818.
- (26) Dewar, M. J. S.; Dougherty, R. C. *The PMO Theory of Organic Chemistry*, 1st ed.; Plenum: New York, 1975.
- (27) Feibelman, P. *Phys. Rev. B* **2008**, *77*, 165419.
- (28) Kresse, G.; Furthmüller, J. *Comput. Mater. Sci.* **1996**, *6*, 15.
- (29) Kresse, G.; Furthmüller, J. *Phys. Rev. B* **1996**, *54*, 11169.
- (30) Blöchl, P. E. *Phys. Rev. B* **1994**, *50*, 17953.
- (31) Kresse, G.; Joubert, D. *Phys. Rev. B* **1999**, *59*, 1758.
- (32) Perdew, J. P.; Burke, K.; Ernzerhof, M. *Phys. Rev. Lett.* **1996**, *77*, 3865.
- (33) Lee, H.; Son, Y.-W.; Park, N.; Han, S.; Yu, J. *Phys. Rev. B* **2005**, *72*, 174431.
- (34) Chernozatonskii, L. A.; Sorokin, P. B.; Bruning, J. W. *Appl. Phys. Lett.* **2007**, *91*, 183103.
- (35) Pisani, L.; Chan, J. A.; Montanari, B.; Harrison, N. M. *Phys. Rev. B* **2007**, *75*, 064418.
- (36) Ryu, S.; Han, M. Y.; Maultzsch, J.; Heinz, T. F.; Kim, P.; Steigerwald, M. L.; Brus, L. E. *Nano Lett.* **2008**, *8*, 4597.
- (37) Elias, D. C.; Nair, R. R.; Mohiuddin, T. M. G.; Morozov, S. V.; Blake, P.; Halsall, M. P.; Ferrari, A. C.; Boukhvalov, D. W.; Katsnelson, M. I.; Geim, A. K.; Novoselov, K. S. *Science* **2009**, *323*, 610.

NL803622C